Producing Gold at ISOLDE-CERN

A.E. Barzakh[a,*], A.N. Andreyev[b,c], D. Atanasov[d,1], J.G. Cubiss[b], R.D. Harding[b,e], M. Al Monthery[b], N.A. Althubiti[f,g], B. Andel[h,i],
S. Antalic[h], J. Ballof[e,j], K. Blaum[d], T.E. Cocolios[f,i], P. Van Duppen[i], T. Day Goodacre[f,e,2], A. de Roubin[d,3], C. Duchemin[e,i],
G.J. Farooq-Smith[f,i,4], D.V. Fedorov[a], V.N. Fedosseev[e], D.A. Fink[d,e], L.P. Gaffney[e,k], L. Ghys[i,l], M. Huyse[i], N. Imai[m], J. Johnson[i],
S. Kreim[d,e], D. Lunney[n,5], K.M. Lynch[f,e], V. Manea[d,5], B.A. Marsh[e], Y. Martinez Palenzuela[i,e], P.L. Molkanov[a], D. Neidherr[o],
V.N. Panteleev[a], M. Rosenbusch[p,6], R.E. Rossel[e,q], S. Rothe[e,q], L. Schweikhard[p], M.D. Seliverstov[a], S. Sels[i], C. Van Beveren[i],
E. Verstraelen[i], A. Welker[e,r], F. Wienholtz[e,p,7], R.N. Wolf[d,p,8], K. Zuber[r]

[a]Petersburg Nuclear Physics Institute, NRC Kurchatov Institute, 188300 Gatchina, Russia
[b]Department of Physics, University of York, York, YO10 5DD, United Kingdom
[c]Advanced Science Research Center (ASRC), Japan Atomic Energy Agency (JAEA), Tokai-mura, Japan
[d]Max-Planck-Institut für Kernphysik, Saupfercheckweg 1, 69117 Heidelberg, Germany
[e]CERN, CH-1211 Geneva 23, Switzerland
[f]The University of Manchester, School of Physics and Astronomy, Oxford Road, M13 9PL Manchester, United Kingdom
[g]Physics Department, College of Science, Jouf University, Sakaka, Kingdom of Saudi Arabia.
[h]Department of Nuclear Physics and Biophysics, Comenius University in Bratislava, 84248 Bratislava, Slovakia
[i]KU Leuven, Instituut voor Kern- en Stralingsfysica, B-3001 Leuven, Belgium
[j]Institut für Kernchemie, Johannes Gutenberg Universität, Fritz-Strassmann-Weg 2, 55128 Mainz, Germany
[k]Department of Physics, University of Liverpool, Liverpool, L69 7ZE, United Kingdom
[l]Belgian Nuclear Research Center SCK CEN, Boeretang 200, B-2400 Mol, Belgium
[m]Center for Nuclear Study (CNS), Graduate School of Science The University of Tokyo, Japan
[n]CSNSM-IN2P3, Université de Paris Sud, Orsay, France
[o]GSI Helmholtzzentrum für Schwerionenforschung GmbH, Darmstadt 64291, Germany
[p]Universität Greifswald, Institut für Physik, 17487 Greifswald, Germany
[q]Institut für Physik, Johannes Gutenberg Universität, D-55099 Mainz, Germany
[r]Institut für Kern- und Teilchenphysik, Technische Universität Dresden, Dresden 01069, Germany

Abstract

The yield of 18 ion beams of radioactive gold nuclei produced in the thick uranium target at ISOLDE (CERN) by 1.4-GeV protons was measured. The production-efficiency dependence on the half-life (efficiency curve) was derived using the in-target production calculations by the FLUKA-CERN code. The irregularities in the efficiency curve for long-lived high-spin gold isomers (^{187,191,193}Au^m) were found. Three release models were tested for the efficiency-curve description.

Keywords: ISOLDE, yield, FLUKA, production efficiency

1. Introduction

Isotope separation on-line (ISOL) facilities exploit thick targets to produce radioactive isotope beams which are used for studies of fundamental nuclear properties and for other purposes such as material science and nuclear medicine applications [1].

Typically in the thick-target ISOL method which is the subject of this paper, high-energy (hundreds of MeV and more) proton beams impinge on targets to induce a wide range of nuclear reactions, producing a large variety of stable and radioactive isotopes. Those isotopes are subsequently extracted from the target matrix by diffusion at high temperature, transported to the ion source (effusion process), ionized, accelerated to energies of $10 - 100$ keV, and finally separated by their mass-to-charge ratio through a dipole magnet. The range of elements is crucially dependent on specific chemical and thermodynamic properties, which define the release pattern from the target. In the best case, the isotopes with half-lives down to a few milliseconds can be delivered to experiments [2].

The knowledge of the yields of the radioactive isotopes at ISOL installations plays a key role in preparing and planning future experiments. It is therefore important to develop ade-

*Corresponding author.
Email address: barzakh_ae@pnpi.nrcki.ru (A.E. Barzakh)
[1]Present address: CERN, 1211, Geneva 23, Switzerland.
[2]Present address: Accelerator Division, TRIUMF, Vancouver BC V6T 2A3, Canada.
[3]Present address: Centre d'Etudes Nucléaires de Bordeaux-Gradignan, 19 Chemin du Solarium, CS 10120, F-33175 Gradignan, France.
[4]Present address: Department of Oncology Physics, Edinburgh Cancer Centre, Western General Hospital, Crewe Road South, Edinburgh, EH4 2XU, United Kingdom.
[5]Present address: Université Paris-Saclay, CNRS/IN2P3, IJCLab, 91405 Orsay, France.
[6]Present address: Wako Nuclear Science Center (WNSC), Institute of Particle and Nuclear Studies (IPNS), High Energy Accelerator Research Organization (KEK), Wako, Saitama 351-0198, Japan
[7]Present address: Institut für Kernphysik, Technische Universität Darmstadt, 64289 Darmstadt, Germany.
[8]Present address: ARC Centre of Excellence for Engineered Quantum Systems, School of Physics, The University of Sydney, NSW 2006, Australia.

quate models that enable the yields of isotopes with unknown production rates to be estimated. To check the reliability of these models and to improve their predictability, they need to be validated with experimental production yields. Comprehensive yield databases exist for more than 70 elements from two thick-target ISOL facilities: ISOLDE (CERN) [3, 4] and ISAC (TRIUMF) [5].

The ISOLDE database also provides in-target production estimation by means of the ABRABLA [6, 7] and FLUKA-CERN [8, 9, 10] codes. At the same time, extensive efforts are underway to build a self-consistent approach for the description of the release from a thick target (see, for example, Refs. [11, 12, 13, 3, 14, 15] and references therein).

For non-volatile elements (such as Ti, Hf, Ir, Pt etc.), difficulties arise to produce radioactive ion beams using the ISOL technique because of their comparatively long release times from a thick target [16]. As a result, there are marked gaps in the yield information for isotopes of these elements. Gold belongs to this category and until now the yields for only two gold isotopes, ^{201,202}Au, have been reported from ISOLDE [17]. However, to provide a benchmark for testing the release models which were applied primarily to the elements with relatively short release time [12], experimental yields are required.

In the present work we report the yields for 18 radioactive gold nuclei produced in the thick uranium target at ISOLDE by 1.4-GeV protons. The measured yields allowed us to check the consistency of the in-target production predictions by the FLUKA-CERN code and to test the applicability of the different release models.

The investigation presented in this paper is a part of our recent experimental campaign at the ISOLDE facility aimed at the nuclear spectroscopy and shape coexistence studies of the neutron-deficient gold isotopes by means of laser ionization spectroscopy. Partial results were reported in Refs. [18, 19, 20, 21, 22].

2. Experimental details

A detailed description of the experiment can be found in Refs. [18, 22]. The gold nuclei were produced in spallation reactions induced by the 1.4-GeV proton beam from the CERN PS Booster, impinging on a 50-g cm^{-2}-thick UC$_x$ target (#524) of the General Purpose Separator (GPS) of ISOLDE [23]. The target and tantalum ionizer cavity were operated at 2150 °C and 2100 °C, respectively. The reaction products diffused through the target and effused as neutral atoms into the hot cavity of the Resonance Ionization Laser Ion Source (RILIS) [24, 25], where gold atoms were ionized by the laser beams with frequencies tuned to the three-step gold ionization scheme presented in [26]. The ions were then extracted by a 30-keV electrostatic potential and separated according to their mass-to-charge ratio. Following the separation, the ions were transported to either the ISOLTRAP's multireflection time-of-flight mass separator (MR-ToF MS) [27, 28], or to the Windmill (WM) system [29, 30] for photoion monitoring during the laser wavelength scans. The WM was used for weakly produced, α-decaying

isotopes, whereas the MR-ToF MS was applied in the longer-lived, β-decaying cases. The hyperfine structure (hfs) and isotope shift (IS) measurements were made upon the 267.7-nm atomic transition in gold ($6s\ ^2S_{1/2} \rightarrow 6p\ ^2P_{1/2}$), by scanning a frequency-tripled Titanium: Sapphire laser in a narrowband mode (bandwidth of $\approx$ 600 MHz before tripling). Two broadband dye lasers (bandwidth of $\approx$ 20 GHz) were used for the second and third excitation steps. Details of the scanning procedures can be found in Refs. [18, 22, 30].

At the WM, the ion beam entered through the central hole of an annular silicon detector (Si1), and was implanted into one of ten, 20 μg cm^{-2}-thick carbon foils mounted on a rotatable wheel. A second silicon detector (Si2) was positioned a few millimeters behind the foil being irradiated. Together, Si1+Si2 were used to measure the short-lived α-decay activity at the implantation site. The typical Si1+Si2 α-detection efficiency was 25 – 40% depending on the specific experimental conditions.

At the MR-ToF MS, separation of the gold ions from isobaric contaminants was achieved due to their mass difference, which resulted in their temporal separation during 1000 revolutions between the electrostatic mirrors of the device. The ions were then extracted from the cavity of the MR-ToF MS and detected with an electron multiplier. Details of the ISOLTRAP apparatus were extensively covered in Refs. [28, 22]. The total transport efficiency between the ISOLDE GPS front end and the MR-ToF MS analysis detector was estimated to be 1% [22]. With direct ion detection and mass-resolving powers in the order of 10^5, this method offers the advantage being independent of the decay properties of the nuclei under investigation.

Yields of short-lived isotopes measured at the end of the run, coincide in the limit of uncertainties with that obtained at the beginning of the experiment. Thus, we did not observe the target aging.

3. Experimental results

In Fig. 1 and Table 1 the yields of the investigated gold isotopes are shown. They are linearly normalized to a proton current of 1 μA (the proton current during the measurements was varied between $1.6 - 2\ \mu$A). Note, that all measurements were done in the narrow-band mode of the RILIS installation. This means that the yields can be increased by a factor of $2 - 3$ when using RILIS in broad-band mode [31]. We preferred not to compare directly the ^{201,202}Au yields from [17] with our data as the experimental conditions in the earlier experiment differ substantially from those of the present work (broad-band RILIS mode, different target thickness, different ionizer type etc.)

For ^{178,177,176}Au^{g,m} the data obtained by the WM decay station were used. The yields were deduced from the α-decay count rate (Si1+Si2) at laser frequencies tuned to the maxima of the hfs, accounting for the α-decay branching ratio, relative intensity of the chosen α line and efficiency of the α-decay detection at the WM (see Refs. [19, 32, 21] and references therein). For the gold nuclei with $A \geq 178$ the hfs spectra measured by the MR-ToF MS were analyzed accounting for the aforementioned transport and detection efficiency.
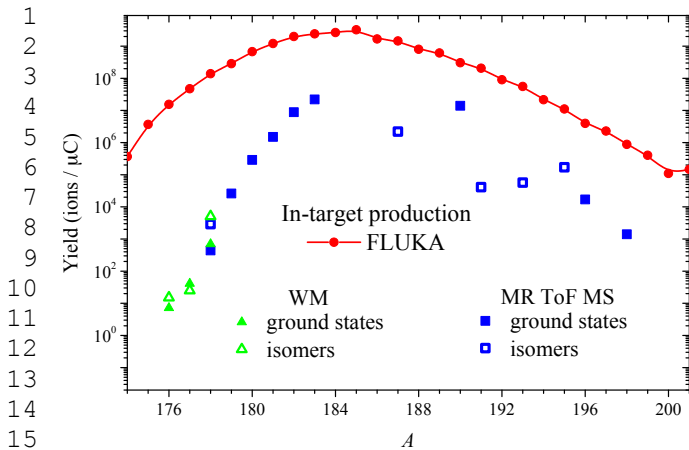
Figure 1: Yields of gold isotopes measured in this study in narrow-band RILIS mode. Upward triangles and squares represent the WM and MR-ToF measurements, respectively. Full and hollow symbols correspond to ground states and isomers, respectively. Circles show the in-target production predicted by the FLUKA-CERN model.

Yields of ^{178}Au^{g,m} were deduced by both procedures. The results obtained from the WM data are in agreement with those from MR-ToF MS measurements within a factor of two (see Fig. 1). This indicates the reliability of the applied procedures and gives an estimation of the yield systematic uncertainties. In Table 1 the yields of ^{178}Au^{g,m} from MR-ToF MS measurements are presented. The yield of ^{190}Au was determined by direct photoion-current measurement with a Faraday cup.

The irregularities in the yields at $A = 187, 191, 193$ (see Fig. 1) are explained by the comparatively short half-lives of the isomers studied at these mass settings in comparison with the half-lives of the corresponding ground states (we did not measure the long-lived ground states of ^{187,191,193}Au since their IS and hfs were investigated previously, see Ref. [33] and references therein). For example, $T_{1/2}(^{191}$Au$^g) = 3.18$ h and $T_{1/2}(^{191}$Au$^m) = 0.92$ s.

Calculations with the FLUKA model were made in the present work with the "FLUKA CERN version 4.1" code [8, 9, 10] (see Fig. 1). For that purpose, a full ISOLDE target unit was modelled and exposed to a proton beam of 1.4 GeV with a Gaussian spatial distribution (with standard deviation of 3.5 mm). The beam and target parameters were based on the experimental values. The irradiated container (cylinder of 0.7 cm radius and 19.5 cm length) of the target unit was filled with UC$_x$ material (with the following weight fractions: ^{235}U − 0.28%, ^{238}U − 82.7%, Carbon − 17.0%) with an apparent density of 3.5 g cm^{-3} as used during the experiment. During the simulation, the residual nuclei yield was computed taking into account the full evolution of the secondary particle cascade. For the production of isomers, FLUKA uses equal-sharing between the ground and the excited states as the first-order approximation. However, this approximation is very crude: we know that sometimes isomer ratio can reach $10 − 10^2$. Therefore, we use total in-target production values, without division on existing isomers. This approach along with the procedure outlined be-

low (see Sec. 4.5), enables one in some cases to determine the experimental values of an isomer ratio rather than to rely upon its theoretical predictions.

The difference between the measured yields and predicted in-target production values reflects the efficiency of the laser-ionization scheme which is the same for all gold isotopes, and the decay losses during the release process which depend on the nuclear half-life.

Table 1: Yields of gold isotopes at ISOLDE measured in this study.

A	$T_{1/2}$	I^a	Yield (ions/μC)
176(m1)	1.36 s	hs	1.5E+01
176(m2)	1.05 s	ls	7.2E+00
177(g)	1.5 s	1/2	4.1E+01
177(m)	1.19 s	(11/2)	2.5E+01
178(g)	3.4 s	ls	4.4E+02
178(m)	2.7 s	hs	2.9E+03
179	7.1 s	1/2	2.6E+04
180	8.1 s	(1)	2.9E+05
181	13.7 s	(3/2)	1.5E+06
182	15.5 s	(2)	8.8E+06
183	42.8 s	(5/2)	2.2E+07
187(m)	2.3 s	9/2	2.2E+06
190	42.8 min	1	1.4E+07
191(m)	0.92 s	(11/2)	4.1E+04
193(m)	3.9 s	11/2	5.7E+04
195(m)	30.5 s	11/2	1.7E+05
196(g)	6.2 d	2	1.7E+04
198(g)	2.7 d	2	1.4E+03

^{a} For isotopes with unknown spin the designation ls (low spin) and hs (high spin) was applied (see Refs. [32, 21]). Spins indicated between brackets are tentative.

4. Description of production efficiency

The ratio of the experimentally observed yield, $Y_{\exp}(^A$Au), and the in-target production, $Y_{\text{in−target}}(^A$Au), will be denoted as a production efficiency, $\epsilon_{\text{tot}} = Y_{\exp}(^A$Au)$/Y_{\text{in−target}}(^A$Au). Several models exist to describe the release process and, in particular, the production efficiency of the radioactive species from the target (see also [3] and references therein).

4.1. Model A

The diffusion-effusion (DE) model is based on the solution of the diffusion equations (see Refs. [34, 35, 11, 13]). In this model the production efficiency of an isotope with a half-life $T_{1/2}$ can be presented as follows:

$$\epsilon_{\text{tot}}(T_{1/2}) = \epsilon_{\text{diff}}(T_{1/2})\epsilon_{\text{eff}}(T_{1/2})\epsilon_{\text{ioniz}}, \quad (1)$$

where $\epsilon_{\text{diff}}, \epsilon_{\text{eff}}, \epsilon_{\text{ioniz}}$ are the diffusion, effusion and ionization efficiencies.

Diffusion and effusion efficiencies depend on the diffusion and effusion time constants t_d and t_e [34, 35]:

3

$$\epsilon_{\text{eff}} = \frac{T_{1/2}}{T_{1/2} + t_e}, \qquad (2)$$

$$\epsilon_{\text{diff}} = 3\delta^{1/2}\left[\coth(\delta^{-1/2}) - \delta^{1/2}\right], \qquad (3)$$

where $\delta = T_{1/2}/(\pi^2 t_d)$.

4.2. Model B

In Ref. [12] an empirical function for the description of the dependence of the production efficiency on the isotope half-life was proposed and successfully applied to a large number of isotopic chains:

$$\epsilon_{\text{tot}}(T_{1/2}) = \epsilon_{\text{ioniz}} \frac{1}{1 + \left(\frac{T_{1/2}}{t_0}\right)^{-\alpha}}. \qquad (4)$$

where α and t_0 are adjustable parameters.

This function may be considered as a simplified version of the DE relations: at $\alpha = 1$ it coincides with $\epsilon_{\text{eff}}\epsilon_{\text{ioniz}}$, at $\alpha \approx 1.5$ it closely approximates $\epsilon_{\text{diff}}\epsilon_{\text{eff}}\epsilon_{\text{ioniz}}$. Its advantage is the decrease of the number of free parameters which is essential in the case of limited experimental information.

4.3. Model C

The third approach is based on the empirical delay function $p(t)$ describing the probability that a stable isotope produced by the protons at $t = 0$ is released at time t [36] :

$$p(t) = \frac{1}{N}\left(1 - e^{-\lambda_r t}\right)\left[\gamma e^{-\lambda_f t} + (1 - \gamma)e^{-\lambda_s t}\right], \qquad (5)$$

where N is a normalizing coefficient, $\lambda_r, \lambda_f, \lambda_s$ are related to the rise, fast-fall and slow-fall time constants t_r, t_f, t_s [$\lambda_r = \ln(2)/t_r$ etc.] and γ is a weighting factor between the slow and fast release components. This four-parameter function satisfactorily describes the experimental release curves whereby the yield was measured as a function of time elapsed after the proton beam pulse impinged on a target. In our analysis we neglect the fast component (i. e. we assume that $\gamma \equiv 0$) since the fluctuations of the experimental points and the lack of the data for isotopes with $T_{1/2} <1$ s do not allow a reasonable fit of a function with so many free parameters.

Then, the production efficiency for radioactive isotope is given by:

$$\epsilon_{\text{tot}} = \epsilon_{\text{ioniz}} \int_0^\infty p(t)e^{-\lambda t}\,dt = \epsilon_{\text{ioniz}} \frac{\lambda_s(\lambda_r + \lambda_s)}{(\lambda + \lambda_s)(\lambda + \lambda_s + \lambda_r)}, \quad (6)$$

where $\lambda = \ln(2)/T_{1/2}$.

In the data fitting by various models we used chi-squared minimization procedure performed with a Levenberg-Marquardt algorithm.
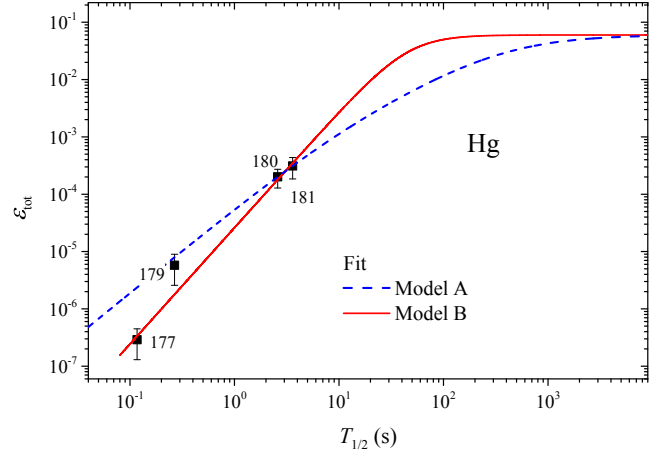

Figure 2: Production efficiency of the neutron deficient mercury isotopes from the UC$_x$ target. Yields were taken from [37]. In-target production was calculated by the FLUKA-CERN code. Fits by Models A (diffusion and effusion) and B are shown by dashed and full lines, respectively.

4.4. Accounting for the parent in-target decay

The production efficiency $\epsilon_{\text{tot}}(T_{1/2})$ depends on the ionization efficiency ϵ_{ioniz}, which is the same for all isotopes and on the decay losses due to the finite decay time. Evidently, ϵ_{tot} should be a smooth function of $T_{1/2}$.

However, there are several factors which might cause irregularities in the experimental data. First of all, the neutron-deficient gold isotopes studied in this work can be produced in the target by the β^+/EC decay of the isobaric mercury precursors. Indeed, the in-target production of mercury isotopes is comparable with or larger than that of the isobaric gold isotopes at $A > 183$. Thus, in these cases the influence of the parent in-target decay might be, in principle, non-negligible. The fraction of the mercury isotopes which decay in the target, depends on the release efficiency for these isotopes. The observed yield of the gold isotope ^{A}Au, $Y(^A\text{Au})_{\text{obs}}$, consists of two parts: ions of gold, produced by the direct reaction in the target, $Y(^A\text{Au})_{\text{direct}}$, and ions of gold, produced by the in-target β decay of the isobaric mercury isotopes, $Y(^A\text{Au})_{\text{decay}}$:

$$Y(^A\text{Au})_{\text{obs}} = Y(^A\text{Au})_{\text{direct}} + Y(^A\text{Au})_{\text{decay}} =$$

$$Y(^A\text{Au})_{\text{in-target}}\epsilon_{\text{tot}}(^A\text{Au}) + \left[1 - \frac{\epsilon_{\text{tot}}(^A\text{Hg})}{\epsilon_{\text{ioniz}}(\text{Hg})}\right] Y(^A\text{Hg})_{\text{in-target}}\epsilon_{\text{tot}}(^A\text{Au}).$$

$$(7)$$

In order to estimate the possible contribution of the mercury in-target decay, we evaluated the production efficiency for mercury isotopes. Yield information for the selected mercury isotopes ($A = 177, 178, 180, 181$) produced in the UC$_x$ target was taken from Ref. [37], and the in-target production was calculated by the FLUKA-CERN code. Note, that temperature parameters during the yield measurements for mercury isotopes were the same as in the present study.

The production efficiencies for mercury isotopes are shown in Fig. 2. The dependence of ϵ_{tot} on $T_{1/2}$ was fitted by Eq. (1)

4

and Eq. (4) (Models A and B, respectively) with the ionization efficiency fixed according to the off-line measurements in Ref. [38], $\epsilon_{\text{ioniz}} = 0.06$. As seen in Fig. 2 the diffusion-effusion model noticeably underestimates the speed of decrease of the production efficiency for short-lived isotopes, whereas empirical Model B satisfactorily describes the experimental data.

We estimated $Y(^A\text{Au})_{\text{decay}}$ with deduced release parameters [Model B: $t_0 = 45(14)$ s, $\alpha = 2.0(2)$]. It contributes $\approx 30\%$ of the total yield for $^{181,182,183}\text{Au}$, 10% for ^{180}Au and less than 1% for other gold isotopes. The corresponding corrections were taken into account in the efficiency-curve analysis. The possible variation of the mercury ionization efficiency ϵ_{ioniz} in the limits of a factor of two, will lead to only a negligible change of this contribution (less than 1%).

Another source of the in-target decay is the α decay of thallium isotopes with 4 more mass units. However, this would only be possible for the lightest isotopes in our data set, for which the production of thallium is at most comparable to that of gold. Considering the small α-decay branching ratio for these thallium isotopes, the impact of these in-target decays will be even less than in the case of mercury. Thus, one can neglect the influence of the parent in-target α decays on the production efficiency of the studied gold isotopes.

4.5. Accounting for the presence of the long-lived isomers

As seen in Table 1, at $A = 176, 177, 178$ the yields of both ground and long-lived isomeric states were independently determined. However, calculation of the in-target production gives the sum of the production rates for all long-lived states of the nucleus in question. One cannot simply add the measured yields of the ground and isomeric states, since they have different half-lives and, correspondingly, different production efficiencies $\epsilon_{\text{tot}}(T_{1/2,g})$ and $\epsilon_{\text{tot}}(T_{1/2,m})$:

$$Y(^A\text{Au}^g) = Y_{\text{in-target}}(^A\text{Au})\beta\epsilon_{\text{tot}}(T_{1/2,g}), \qquad (8)$$

$$Y(^A\text{Au}^m) = Y_{\text{in-target}}(^A\text{Au})(1 - \beta)\epsilon_{\text{tot}}(T_{1/2,m}), \qquad (9)$$

where β is the (unknown) fraction of ^AAu nuclei in ground state, produced by spallation reaction in the UC$_x$ target. Thus, the respective production efficiency can be determined by the iterative procedure with the relation derived from Eq. (9) after substitution of β from Eq. (8):

$$\epsilon_{\text{tot}}(T_{1/2,g}) = \left[Y(^A\text{Au}^g) + Y(^A\text{Au}^m)\frac{\epsilon_{\text{tot}}(T_{1/2,g})}{\epsilon_{\text{tot}}(T_{1/2,m})}\right] / Y_{\text{in-target}}. \qquad (10)$$

Namely, the production efficiency dependence on $T_{1/2}$ should be fitted without taking into account the yield for the ^AAu nucleus. Then the ratio $\frac{\epsilon_{\text{tot}}(T_{1/2,g})}{\epsilon_{\text{tot}}(T_{1/2,m})}$ should be calculated with the obtained release parameters. Inserting this ratio in Eq. (10), one obtains $\epsilon_{\text{tot}}(T_{1/2}, g)$. This value should be included in the next iteration of the fitting procedure and so on until a self-consistent result is obtained. Note, that Eqs. (8, 9, 10) are valid only when internal transitions are absent. This is the case for $^{176,177,178}\text{Au}^m$.

5. Production efficiency for neutron-deficient gold isotopes

5.1. General considerations

In Fig. 3 the production efficiency of the studied ground and isomeric states of gold isotopes is presented as a function of the half-life of the corresponding nuclei.
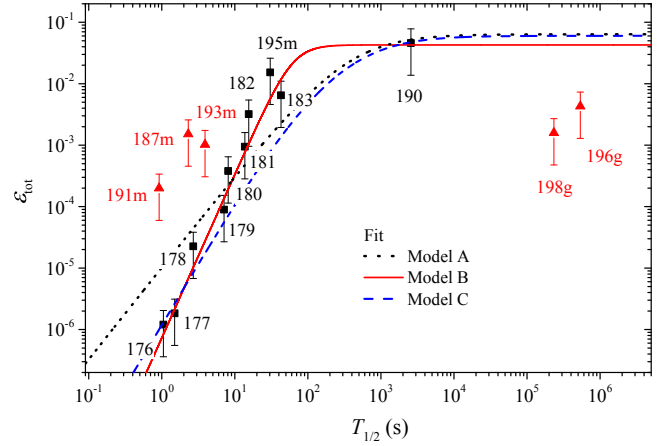

Figure 3: Production efficiency of the gold isotopes released from the thick UC$_x$ target, when the in-target production was calculated with the FLUKA-CERN code. The data for $^{187,191,193,196,198}\text{Au}$ were not included in the fits (see text for details). Fits by the Model A, B and C are shown by dotted, full and dashed lines, respectively.

One can see that in Fig. 3 all points but those for $^{187,191,193,196,198}\text{Au}$ follow the same systematic trend. The deviation for $^{196,198}\text{Au}^g$ can be explained by the presence of long-lived high-spin isomers in these nuclei ($^{196}\text{Au}^m$, $T_{1/2} = 9.6$ h, $I = 12$; $^{198}\text{Au}^m$, $T_{1/2} = 2.3$ d, $I = 12$). The behavior of the $^{196,198}\text{Au}^g$ production efficiencies may be regarded as an indication that the yields of the corresponding long-lived high-spin isomers are larger than those for the low-spin ground states by at least a factor of ten. In this case one can expect that after adding the production efficiencies of these isomers to the measured efficiencies of the ground states (taking into account the difference in the half-lives as shown in Sec. 4.5) the drop of the $^{196,198}\text{Au}^g$ points will disappear. Note, that ^{190}Au also has a high-spin isomer ($T_{1/2} = 125$ ms, $I = 11$), but due to its short half-life and the predominance of the IT branch, it decays almost completely to the low-spin ground state in the target and the observed production efficiency of $^{190}\text{Au}^g$ comprises the sum of the production efficiencies of both isomer and ground state. Correspondingly, there is no marked deviation from the common trend for $^{190}\text{Au}^g$. In the fitting procedures, the (incomplete) data for $^{196,198}\text{Au}^g$ were ignored.

However, there are three additional points outside the common trend ($A = 187, 191, 193$) in the efficiency curve (see Fig. 3). The deviation of these points from the systematic trend amounts to a factor of 220 for ^{187}Au, a factor of 290 for ^{191}Au and a factor of 40 for ^{193}Au. Note, that accounting for the yield of the ground states of these nuclei (which were not measured in our experiment) would increase this deviation. The additional experimental and theoretical studies are needed in order to explain the observed irregularities.

5.2. Comparison with theoretical models

Despite the clear irregularities in the efficiency curve at $A =$ 187, 191, 193 (see Fig. 3), the data for other isotopes (apart from ^{187,191,193,196,198}Au) are described well by the Model B with the following parameters: $\epsilon_{\mathrm{ioniz}} = 0.04(2)$, $t_0 = 73(21)$ s, $\alpha = 2.5(2)$ (see Fig. 3). The obtained ionization efficiency matches well with the off-line estimation $\epsilon_{\mathrm{ioniz}}(\mathrm{Au}) > 0.03$ [26]. At the same time Model A ($\epsilon_{\mathrm{ioniz}} = 0.06$, $t_r = 100$ s, $t_s = 600$ s) noticeably underestimates the slope of the efficiency curve for the short-lived gold isotopes, whereas Model C ($\epsilon_{\mathrm{ioniz}} = 0.06$, $t_{\mathrm{diff}} = 400$ s, $t_{\mathrm{eff}} = 300$ s) poorly describes the "intermediate" isotopes with 10 s $< T_{1/2} < 100$ s.

6. Conclusions

To summarize, the production yield of radioactive ion beams for 18 gold nuclei produced in the thick uranium target at ISOLDE by 1.4-GeV protons and ionized by RILIS, were measured. The production-efficiency dependence on the half-life was established by using the FLUKA-CERN in-target production values. The deviations from the common trend of this dependence for ^{196,198}Au were explained by the assumption of the stronger production of the long-lived high-spin isomers in comparison with their low-spin ground states.

On the other hand, the observed irregularities in the ϵ_{tot} half-life dependence for the long-lived high-spin gold isomers ($A = 187, 191, 193$) demand additional experimental and theoretical efforts in order to explain this deviation and establish reliable release model. First of all, yield measurements for gold should be continued with special emphasis on the isotopes having long-lived isomer states. It would be important to fill the gaps in our data ($183 < A < 198$) in order to check the consistency of the theoretical prediction in the specific mass region. It would be instructive also to compare the FLUKA results with the predictions of other transport codes. Measuring the release curve could further improve our understanding of the processes involved and predictions for other nuclides.

References

[1] Y. Blumenfeld, T. Nilsson, P. Van Duppen, Facilities and methods for radioactive ion beam production, Phys. Scripta T 152 (2013) 014023. doi:10.1088/0031-8949/2013/T152/014023.

[2] M. J. G. Borge, B. Jonson, ISOLDE past, present and future, J. Phys. G 44 (4) (2017) 044011, [Erratum: J.Phys.G 44, 079501 (2017)]. doi:10.1088/1361-6471/aa5f03.

[3] J. Ballof, J. Ramos, A. Molander, K. Johnston, S. Rothe, T. Stora, C. Düllman, The upgraded ISOLDE yield database - a new tool to predict beam intensities, Nucl. Instrum. Methods Phys. Res. B 463 (2019) 211. doi:https://doi.org/10.1016/j.nimb.2019.05.044.
URL https://www.sciencedirect.com/science/article/pii/S0168583X19303659

[4] The ISOLDE Yield Database, Version 0.1, https://cern.ch/isolde-yields, [Online; accessed 04.04.2021] (2020).

[5] P. Kunz, et al., ISAC Yield Database, https://mis.triumf.ca/science/planning/yield/beam, [Online; accessed 04.04.2021] (2020).

[6] K.-H. Schmidt, M. Ricciardi, A. Botvina, T. Enqvist, Production of neutron-rich heavy residues and the freeze-out temperature in the fragmentation of relativistic ^{238}U projectiles determined by the isospin thermometer, Nucl. Phys. A 710 (1) (2002) 157. doi:https://doi.org/10.1016/S0375-9474(02)01120-X.
URL https://www.sciencedirect.com/science/article/pii/S037594740201120X

[7] A. Kelić, M. Ricciardi, K.-H. Schmidt, Abla07 - towards a complete description of the decay channels of a nuclear system from spontaneous fission to multifragmentation, in: D. Filges, S. Leray, Y. Yariv, A. Mengoni, A. Stanculescu, G. Mank (Eds.), Joint ICTP-IAEA Advanced Workshop on Model Codes for Spallation Reactions Trieste, Italy, February 4-8, 2008, 2008, p. 181.
URL http://www-nds.iaea.org/reports-new/indc-reports/indc-nds/indc-nds-0530.pdf

[8] FLUKA-CERN Website, https://fluka.cern, [Online; accessed 04.03.2021] (2020).

[9] T. Böhlen, F. Cerutti, M. Chin, A. Fassò, A. Ferrari, P. Ortega, A. Mairani, P. Sala, G. Smirnov, V. Vlachoudis, The FLUKA code: Developments and challenges for high energy and medical applications, Nuclear Data Sheets 120 (2014) 211–214. doi:https://doi.org/10.1016/j.nds.2014.07.049.
URL https://www.sciencedirect.com/science/article/pii/S0090375214005018

[10] G. Battistoni, T. Boehlen, F. Cerutti, P. W. Chin, L. S. Esposito, A. Fassò, A. Ferrari, A. Lechner, A. Empl, A. Mairani, A. Mereghetti, P. G. Ortega, J. Ranft, S. Roesler, P. R. Sala, V. Vlachoudis, G. Smirnov, Overview of the FLUKA code, Annals of Nuclear Energy 82 (2015) 10–18, Joint International Conference on Supercomputing in Nuclear Applications and Monte Carlo 2013, SNA + MC 2013. Pluri- and Trans-disciplinarity, Towards New Modeling and Numerical Simulation Paradigms. doi:https://doi.org/10.1016/j.anucene.2014.11.007.
URL https://www.sciencedirect.com/science/article/pii/S0306454914005878

[11] J. Bennett, Delays in thick targets, Nucl. Phys. A 701 (1) (2002) 296. doi:https://doi.org/10.1016/S0375-9474(01)01602-5.
URL https://www.sciencedirect.com/science/article/pii/S0375947401016025

[12] S. Lukić, F. Gevaert, A. Kelić, M. Ricciardi, K.-H. Schmidt, O. Yordanov, Systematic comparison of ISOLDE-SC yields with calculated in-target production rates, Nucl. Instrum. Methods Phys. Res. A 565 (2) (2006) 784. doi:https://doi.org/10.1016/j.nima.2006.04.082.
URL https://www.sciencedirect.com/science/article/pii/S0168900206007005

[13] A. E. Barzakh, G. Lhersonneau, L. K. Batist, D. V. Fedorov, V. S. Ivanov, K. A. Mezilev, P. L. Molkanov, F. V. Moroz, S. Y. Orlov, V. N. Panteleev,

6

Y. M. Volkov, O. Alyakrinskiy, M. Barbui, L. Stroe, L. B. Tecchio, Secondary neutrons as the main source of neutron-rich fission products in the bombardment of a thick U target by 1 GeV protons, Eur. Phys. J. A 47 (5) (2011) 70. doi:10.1140/epja/i2011-11070-y.
URL https://doi.org/10.1140/epja/i2011-11070-y

[14] T. E. Cocolios, B. A. Marsh, V. N. Fedosseev, S. Franchoo, G. Huber, M. Huyse, A. M. Ionan, K. Johnston, U. Köster, Y. Kudryavtsev, M. Seliverstov, E. Noah, T. Stora, P. Van Duppen, Resonant laser ionization of polonium at rilis-isolde for the study of ground- and isomer-state properties, Nucl. Instrum. Methods Phys. Res. B 266 (19) (2008) 4403–4406, proceedings of the XVth International Conference on Electromagnetic Isotope Separators and Techniques Related to their Applications. doi:https://doi.org/10.1016/j.nimb.2008.05.142.
URL https://www.sciencedirect.com/science/article/pii/S0168583X08007453

[15] T. Stora, E. Noah, R. Hodak, T. Y. Hirsh, M. Hass, V. Kumar, K. Singh, S. Vaintraub, P. Delahaye, H. Franberg-Delahaye, M.-G. Saint-Laurent, G. Lhersonneau, A high intensity 6 he beam for the β-beam neutrino oscillation facility, EPL (Europhysics Letters) 98 (3) (2012) 32001. doi:10.1209/0295-5075/98/32001.
URL https://doi.org/10.1209/0295-5075/98/32001

[16] U. Köster, P. Carbonez, A. Dorsival, J. Dvorak, R. Eichler, S. Fernandes, H. Frånberg, J. Neuhausen, Z. Novackova, R. Wilfinger, A. Yakushev, (Im-)possible ISOL beams, The European Physical Journal Special Topics 150 (2007) 285. doi:10.1140/epjst/e2007-00326-1.
URL https://doi.org/10.1140/epjst/e2007-00326-1

[17] T. Stora, Recent developments of target and ion sources to produce ISOL beams, Nucl. Instrum. Methods Phys. Res. B 317 (2013) 402. doi:https://doi.org/10.1016/j.nimb.2013.07.024.
URL https://www.sciencedirect.com/science/article/pii/S0168583X13008185

[18] J. Cubiss, A. Barzakh, A. Andreyev, M. Al Monthery, N. Althubiti, B. Andel, S. Antalic, D. Atanasov, K. Blaum, T. Cocolios, T. Day Goodacre, R. de Groote, A. de Roubin, G. Farooq-Smith, D. Fedorov, V. Fedosseev, R. Ferrer, D. Fink, L. Gaffney, L. Ghys, A. Gredley, R. Harding, F. Herfurth, M. Huyse, N. Imai, D. Joss, U. Köster, S. Kreim, V. Liberati, D. Lunney, K. Lynch, V. Manea, B. Marsh, Y. Martinez Palenzuela, P. Molkanov, P. Mosat, D. Neidherr, G. O'Neill, R. Page, T. Procter, E. Rapisarda, M. Rosenbusch, S. Rothe, K. Sandhu, L. Schweikhard, M. Seliverstov, S. Sels, P. Spagnoletti, V. Truesdale, C. Van Beveren, P. Van Duppen, M. Veinhard, M. Venhart, M. Veselský, F. Wearing, A. Welker, F. Wienholtz, R. Wolf, S. Zemlyanoy, K. Zuber, Change in structure between the I = 1/2 states in ^{181}Tl and ^{177,179}Au, Phys. Lett. B 786 (2018) 355. doi:https://doi.org/10.1016/j.physletb.2018.10.005.
URL https://www.sciencedirect.com/science/article/pii/S0370269318307627

[19] R. D. Harding, A. N. Andreyev, A. E. Barzakh, D. Atanasov, J. G. Cubiss, P. Van Duppen, M. Al Monthery, N. A. Althubiti, B. Andel, S. Antalic, K. Blaum, T. E. Cocolios, T. Day Goodacre, A. de Roubin, G. J. Farooq-Smith, D. V. Fedorov, V. N. Fedosseev, D. A. Fink, L. P. Gaffney, L. Ghys, D. T. Joss, F. Herfurth, M. Huyse, N. Imai, S. Kreim, D. Lunney, K. M. Lynch, V. Manea, B. A. Marsh, Y. Martinez Palenzuela, P. L. Molkanov, D. Neidherr, R. D. Page, A. Pastore, M. Rosenbusch, R. E. Rossel, S. Rothe, L. Schweikhard, M. D. Seliverstov, S. Sels, C. Van Beveren, E. Verstraelen, A. Welker, F. Wienholtz, R. N. Wolf, K. Zuber, Laser-assisted decay spectroscopy for the ground states of ^{180,182}Au, Phys. Rev. C 102 (2020) 024312. doi:10.1103/PhysRevC.102.024312.
URL https://link.aps.org/doi/10.1103/PhysRevC.102.024312

[20] A. E. Barzakh, D. Atanasov, A. N. Andreyev, M. Al Monthery, N. A. Althubiti, B. Andel, S. Antalic, K. Blaum, T. E. Cocolios, J. G. Cubiss, P. Van Duppen, T. D. Goodacre, A. de Roubin, Y. A. Demidov, G. J. Farooq-Smith, D. V. Fedorov, V. N. Fedosseev, D. A. Fink, L. P. Gaffney, L. Ghys, R. D. Harding, D. T. Joss, F. Herfurth, M. Huyse, N. Imai, M. G. Kozlov, S. Kreim, D. Lunney, K. M. Lynch, V. Manea, B. A. Marsh, Y. Martinez Palenzuela, P. L. Molkanov, D. Neidherr, R. D. Page, M. Rosenbusch, R. E. Rossel, S. Rothe, L. Schweikhard, M. D. Seliverstov, S. Sels, C. Van Beveren, E. Verstraelen, A. Welker, F. Wienholtz, R. N. Wolf, K. Zuber, Hyperfine anomaly in gold and magnetic moments of $I^{\pi} = 11/2^-$ gold isomers, Phys. Rev. C 101 (2020) 034308. doi:10.1103/PhysRevC.101.034308.
URL https://link.aps.org/doi/10.1103/PhysRevC.101.034308

[21] J. G. Cubiss, A. N. Andreyev, A. E. Barzakh, V. Manea, M. A. Monthery, N. A. Althubiti, B. Andel, S. Antalic, D. Atanasov, K. Blaum, T. E. Cocolios, T. D. Goodacre, A. de Roubin, G. J. Farooq-Smith, D. V. Fedorov, V. N. Fedosseev, D. A. Fink, L. P. Gaffney, L. Ghys, R. D. Harding, F. Herfurth, M. Huyse, N. Imai, D. T. Joss, S. Kreim, D. Lunney, K. M. Lynch, B. A. Marsh, Y. M. Palenzuela, P. L. Molkanov, D. Neidherr, G. G. O'Neill, R. D. Page, M. Rosenbusch, R. E. Rossel, S. Rothe, L. Schweikhard, M. D. Seliverstov, S. Sels, A. Stott, C. Van Beveren, P. Van Duppen, E. Verstraelen, A. Welker, F. Wienholtz, R. N. Wolf, K. Zuber, Laser-assisted decay spectroscopy and mass spectrometry of ^{178}Au, Phys. Rev. C 102 (2020) 044332. doi:10.1103/PhysRevC.102.044332.
URL https://link.aps.org/doi/10.1103/PhysRevC.102.044332

[22] A. E. Barzakh, D. Atanasov, A. N. Andreyev, M. A. Monthery, N. A. Althubiti, B. Andel, S. Antalic, K. Blaum, T. E. Cocolios, J. G. Cubiss, P. Van Duppen, T. D. Goodacre, A. de Roubin, G. J. Farooq-Smith, D. V. Fedorov, V. N. Fedosseev, D. A. Fink, L. P. Gaffney, L. Ghys, R. D. Harding, M. Huyse, N. Imai, S. Kreim, D. Lunney, K. M. Lynch, V. Manea, B. A. Marsh, Y. M. Palenzuela, P. L. Molkanov, D. Neidherr, M. Rosenbusch, R. E. Rossel, S. Rothe, L. Schweikhard, M. D. Seliverstov, S. Sels, C. Van Beveren, E. Verstraelen, A. Welker, F. Wienholtz, R. N. Wolf, K. Zuber, Shape coexistence in ^{187}Au studied by laser spectroscopy, Phys. Rev. C 101 (2020) 064321. doi:10.1103/PhysRevC.101.064321.
URL https://link.aps.org/doi/10.1103/PhysRevC.101.064321

[23] R. Catherall, W. Andreazza, M. Breitenfeldt, A. Dorsival, G. J. Focker, T. P. Gharsa, G. T. J, J.-L. Grenard, F. Locci, P. Martins, S. Marzari, J. Schipper, A. Shornikov, T. Stora, The ISOLDE facility, J. Phys. G: Nucl. Part. Phys. 44 (9) (2017) 094002. doi:10.1088/1361-6471/aa7eba.
URL https://doi.org/10.1088/1361-6471/aa7eba

[24] V. Mishin, V. Fedoseyev, H.-J. Kluge, V. Letokhov, H. Ravn, F. Scheerer, Y. Shirakabe, S. Sundell, O. Tengblad, Chemically selective laser ion-source for the CERN-ISOLDE on-line mass separator facility, Nucl. Instrum. Methods Phys. Res. B 73 (4) (1993) 550. doi:https://doi.org/10.1016/0168-583X(93)95839-W.
URL https://www.sciencedirect.com/science/article/pii/0168583X9395839W

[25] V. Fedosseev, K. Chrysalidis, T. D. Goodacre, B. Marsh, S. Rothe, C. Seiffert, K. Wendt, Ion beam production and study of radioactive isotopes with the laser ion source at ISOLDE, J. Phys. G: Nucl. Part. Phys. 44 (8) (2017) 084006. doi:10.1088/1361-6471/aa78e0.
URL https://doi.org/10.1088/1361-6471/aa78e0

[26] B. Marsh, V. Fedosseev, P. Kosuri, ISOLDE Collaboration, Development of a RILIS ionization scheme for gold at ISOLDE, CERN, Hyperfine Interact. 171 (1) (2006) 109. doi:10.1007/s10751-006-9498-8.
URL https://doi.org/10.1007/s10751-006-9498-8

[27] M. Mukherjee, D. Beck, K. Blaum, G. Bollen, J. Dilling, S. George, F. Herfurth, A. Herlert, A. Kellerbauer, H.-J. Kluge, et al., ISOLTRAP: An on-line Penning trap for mass spectrometry on short-lived nuclides, Eur. Phys. J. A 35 (1) (2008) 1. doi:10.1140/epja/i2007-10528-9.
URL https://doi.org/10.1140/epja/i2007-10528-9

[28] R. Wolf, F. Wienholtz, D. Atanasov, D. Beck, K. Blaum, C. Borgmann, F. Herfurth, M. Kowalska, S. Kreim, Y. A. Litvinov, D. Lunney, V. Manea, D. Neidherr, M. Rosenbusch, L. Schweikhard, J. Stanja, K. Zuber, ISOLTRAP's multi-reflection time-of-flight mass separator/spectrometer, Int. J. Mass Spectrom. 349-350 (2013) 123. doi:https://doi.org/10.1016/j.ijms.2013.03.020.
URL https://www.sciencedirect.com/science/article/pii/S1387380613001115

[29] A. N. Andreyev, J. Elseviers, M. Huyse, P. Van Duppen, S. Antalic, A. Barzakh, N. Bree, T. E. Cocolios, V. F. Comas, J. Diriken, D. Fedorov, V. Fedosseev, S. Franchoo, J. A. Heredia, O. Ivanov, U. Köster, B. A. Marsh, K. Nishio, R. D. Page, N. Patronis, M. Seliverstov, I. Tsekhanovich, P. Van den Bergh, J. Van De Walle, M. Venhart, S. Vermote, M. Veselsky, C. Wagemans, T. Ichikawa,

7

A. Iwamoto, P. Möller, A. J. Sierk, New type of asymmetric fission in proton-rich nuclei, Phys. Rev. Lett. 105 (2010) 252502. doi:10.1103/PhysRevLett.105.252502.
URL https://link.aps.org/doi/10.1103/PhysRevLett.105.252502

[30] M. D. Seliverstov, T. E. Cocolios, W. Dexters, A. N. Andreyev, S. Antalic, A. E. Barzakh, B. Bastin, J. Büscher, I. G. Darby, D. V. Fedorov, V. N. Fedosseev, K. T. Flanagan, S. Franchoo, G. Huber, M. Huyse, M. Keupers, U. Köster, Y. Kudryavtsev, B. A. Marsh, P. L. Molkanov, R. D. Page, A. M. Sjödin, I. Stefan, P. Van Duppen, M. Venhart, S. G. Zemlyanoy, Electromagnetic moments of odd-A $^{193-203,211}$Po isotopes, Phys. Rev. C 89 (2014) 034323. doi:10.1103/PhysRevC.89.034323.
URL https://link.aps.org/doi/10.1103/PhysRevC.89.034323

[31] B. Andel, A. N. Andreyev, S. Antalic, M. Al Monthery, A. Barzakh, M. L. Bissell, K. Chrysalidis, T. E. Cocolios, J. G. Cubiss, T. Day Goodacre, N. Dubray, G. J. Farooq-Smith, D. V. Fedorov, V. N. Fedosseev, L. P. Gaffney, R. F. Garcia Ruiz, S. Goriely, C. Granados, R. D. Harding, R. Heinke, S. Hilaire, M. Huyse, J.-F. Lemaître, K. M. Lynch, B. A. Marsh, P. Molkanov, P. Mosat, S. Péru, C. Raison, S. Rothe, C. Seiffert, M. D. Seliverstov, S. Sels, D. Studer, J. Sundberg, P. Van Duppen, β-delayed fission of isomers in ^{188}Bi, Phys. Rev. C 102 (2020) 014319. doi:10.1103/PhysRevC.102.014319.
URL https://link.aps.org/doi/10.1103/PhysRevC.102.014319

[32] R. D. Harding, J. G. Cubiss, A. N. Andreyev, A. E. Barzakh, V. Manea, M. A. Monthery, N. A. Althubiti, B. Andel, S. Antalic, D. Atanasov, K. Blaum, T. E. Cocolios, T. D. Goodacre, A. de Roubin, G. J. Farooq-Smith, D. V. Fedorov, V. N. Fedosseev, D. A. Fink, L. P. Gaffney, L. Ghys, F. Herfurth, M. Huyse, N. Imai, D. T. Joss, S. Kreim, D. Lunney, K. M. Lynch, B. A. Marsh, Y. M. Palenzuela, P. L. Molkanov, D. Neidherr, G. G. O'Neill, R. D. Page, M. Rosenbusch, R. E. Rossel, S. Rothe, L. Schweikhard, M. D. Seliverstov, S. Sels, A. Stott, C. Van Beveren, P. Van Duppen, E. Verstraelen, A. Welker, F. Wienholtz, R. N. Wolf, K. Zuber, Laser-assisted nuclear decay spectroscopy of ^{176,177,179}Au, Phys. Rev. C 000 (2021) 0, in press.

[33] G. Passler, J. Rikovska, E. Arnold, H.-J. Kluge, L. Monz, R. Neugart, H. Ravn, K. Wendt, Quadrupole moments and nuclear shapes of neutron-deficient gold isotopes, Nucl. Phys. A 580 (2) (1994) 173. doi:https://doi.org/10.1016/0375-9474(94)90769-2.
URL https://www.sciencedirect.com/science/article/pii/0375947494907692

[34] H. Ravn, L. Carraz, J. Denimal, E. Kugler, M. Skarestad, S. Sundell, L. Westgaard, New techniques at ISOLDE-2, Nucl. Instrum. Methods 139 (1976) 267. doi:https://doi.org/10.1016/0029-554X(76)90684-4.
URL https://www.sciencedirect.com/science/article/pii/0029554X76906844

[35] M. Fujioka, Y. Arai, Diffusion of radioisotopes from solids in the form of foils, fibers and particles, Nucl. Instrum. Methods Phys. Res. 186 (1) (1981) 409. doi:https://doi.org/10.1016/0029-554X(81)90933-2.
URL https://www.sciencedirect.com/science/article/pii/0029554X81909332

[36] J. Lettry, R. Catherall, P. Drumm, P. Van Duppen, A. Evensen, G. Focker, A. Jokinen, O. Jonsson, E. Kugler, H. Ravn, Pulse shape of the ISOLDE radioactive ion beams, Nucl. Instrum. Methods Phys. Res. B 126 (1) (1997) 130. doi:https://doi.org/10.1016/S0168-583X(96)01025-7.
URL https://www.sciencedirect.com/science/article/pii/S0168583X96010257

[37] S. Sels, T. Day Goodacre, B. A. Marsh, A. Pastore, W. Ryssens, Y. Tsunoda, N. Althubiti, B. Andel, A. N. Andreyev, D. Atanasov, A. E. Barzakh, M. Bender, J. Billowes, K. Blaum, T. E. Cocolios, J. G. Cubiss, J. Dobaczewski, G. J. Farooq-Smith, D. V. Fedorov, V. N. Fedosseev, K. T. Flanagan, L. P. Gaffney, L. Ghys, P.-H. Heenen, M. Huyse, S. Kreim, D. Lunney, K. M. Lynch, V. Manea, Y. Martinez Palenzuela, T. M. Medonca, P. L. Molkanov, T. Otsuka, J. P. Ramos, R. E. Rossel, S. Rothe, L. Schweikhard, M. D. Seliverstov, P. Spagnoletti, C. Van Beveren, P. Van Duppen, M. Veinhard, E. Verstraelen, A. Welker, K. Wendt, F. Wienholtz, R. N. Wolf, A. Zadvornaya, Shape staggering of midshell

mercury isotopes from in-source laser spectroscopy compared with density-functional-theory and Monte Carlo shell-model calculations, Phys. Rev. C 99 (2019) 044306. doi:10.1103/PhysRevC.99.044306.
URL https://link.aps.org/doi/10.1103/PhysRevC.99.044306

[38] T. D. Goodacre, J. Billowes, K. Chrysalidis, D. Fedorov, V. Fedosseev, B. Marsh, P. Molkanov, R. Rossel, S. Rothe, C. Seiffert, K. D. A. Wendt, RILIS-ionized mercury and tellurium beams at ISOLDE CERN, Hyperfine Interact. 238 (1) (2017) 41. doi:10.1007/s10751-017-1398-6.
URL https://doi.org/10.1007/s10751-017-1398-6

[39] U. Köster, V. Fedoseyev, A. Andreyev, U. Bergmann, R. Catherall, J. Cederkäll, M. Dietrich, H. De Witte, D. Fedorov, L. Fraile, S. Franchoo, H. Fynbo, U. Georg, T. Giles, M. Gorska, M. Hannawald, M. Huyse, A. Joinet, O. Jonsson, K. Kratz, K. Kruglov, C. Lau, J. Lettry, V. Mishin, M. Oinonen, K. Partes, K. Peräjärvi, B. Pfeiffer, H. Ravn, M. Seliverstov, P. Thirolf, K. Van de Vel, P. Van Duppen, J. Van Roosbroeck, L. Weissman, On-line yields obtained with the ISOLDE RILIS, Nucl. Instrum. Methods Phys. Res. B 204 (2003) 347. doi:https://doi.org/10.1016/S0168-583X(02)01956-0.
URL https://www.sciencedirect.com/science/article/pii/S0168583X02019560